Available online at www.sciencedirect.com
ScienceDirect
Earth and Planetary Science Letters 255 (2007) 22–31
EPSL
www.elsevier.com/locate/epsl

Locating scatterers in the mantle using array analysis of PKP precursors from an earthquake doublet

Aimin Cao *, Barbara Romanowicz

Seismological Laboratory, University of California, Berkeley, United States

Received 18 September 2006; received in revised form 30 November 2006; accepted 1 December 2006
Available online 8 January 2007
Editor: R.D. van der Hilst

Abstract

Well separated individual PKP precursors observed at the Yellowknife seismic array (YK) for a high quality doublet of earthquakes provide an opportunity to study the location of the corresponding scatterers and assess the stability of the location estimation. Based on the comparison of the waveforms of stacked individual precursors and those of PKIKP phases, we are able to determine that most of these precursors originate from scattering of the PKPbc (rather than the PKPab) branch above the B caustic on the receiver side. This allows a reliable location of the scatterers in the lower mantle. Their depths range from 2890 km (the CMB) to 2270 km, scattering angles range from 45.8° to 16.0°, and surface projections range from southern Ontario to northern Saskatchewan in Canada. These locations are associated with transitions from slow to fast velocities in mantle tomographic models and follow the expected general dip direction of fossil slabs under north America. This suggests that the subducted slab remnants under north America have retained their compositional signature. The fact that we can essentially treat these scatterers as reflections from plane boundaries suggests that the remnant fragments of slab may be spatially extended, which should be confirmed using broadband data. Average differences in measured slowness and back-azimuth of the doublet precursors are as small as 0.08 s/deg and 1.4 deg, respectively. Our study indicates that it may be possible to locate such scatterers using single earthquakes and small aperture seismic arrays.

Keywords: PKP precursors; scatterers; slowness; back-azimuth

1. Introduction

PKP precursors were first observed in the 1930's [1], but it has taken more than sixty years to establish their origin. Array analyses of arrival times, slownesses, and spectra [2–6] have suggested that these precursors are scattered waves from the lower mantle rather than diffracted, reflected, or refracted waves from the core [7,8]. Global simulations under the single and multiple scattering hypotheses have determined that small-scale, weak ($<\sim 1\%$) heterogeneities distributed throughout the mantle likely contribute to the PKP precursor wavetrains, with perhaps a concentration in the lowermost mantle [9–11].

Small-scale heterogeneities have important geodynamic significance in mantle convection [9,10]. In particular, subducted slabs can survive for billions of years in the lower mantle due to incomplete mixing [12–14], and so regional distributions of small-scale heterogeneity in subduction or upwelling zones might help us sketch out local depth ranges of the mantle flow

* Corresponding author.
E-mail address: acao@seismo.berkeley.edu (A. Cao).

0012-821X/$ - see front matter © 2006 Elsevier B.V. All rights reserved.
doi:10.1016/j.epsl.2006.12.002

field and understand better the distribution and nature of heterogeneity. Given the fact that current resolution provided by seismic tomography is not high enough to image structures at scales of ~1−10 km, locating and estimating the size and strength of individual scatterers responsible for PKP precursors provides a potential complementary approach.

Recent studies have derived general properties of the PKP precursor field from the analysis of high quality data from the global seismic network [9,10,15] or from large aperture seismic arrays [16–18]. The large aperture of the arrays considered prevented the use of standard array processing techniques such as the construction of vespagrams [16]. Even when considering stacks across small-aperture arrays such as Norsar [19], these studies have primarily modelled stacks of the envelopes of the precursor train, and only in a statistical sense. In most cases, these authors have invoked the presence of partial melting associated with Ultra Low Velocity zones to interpret the large velocity contrasts (~10%) necessary to explain the observed precursor amplitudes.

However, very few studies have attempted to locate individual scatterers in the mantle, because PKP precursors are usually weak and their arrivals overlap. Doornbos [6] tried to locate the scattering regions using the NORSAR seismic array, but he pointed out that the uncertainty in the precursor slowness measurements was unknown. The arrival time of the onset of the precursor train has also been used to try and locate the region of observed strong scattering [17,18]. An added complication comes from the fact that there is ambiguity between source and receiver side scattering. In general, this is resolved indirectly, by comparing paths in different azimuths from the source or receiver side, and proposing an interpretation most compatible with all observations. Hedlin and Shearer [20] showed that the ambiguity can be resolved in many regions of the lowermost mantle by inverting a global dataset of precursor average power estimates, in the framework of Rayleigh–Born scattering theory. Finally, even if the slowness and back-azimuth of a precursor can be precisely estimated using a small-aperture seismic array, it is also necessary to know if the precursor was scattered from PKPbc or PKPab on the receiver side or on the source side (Fig. 1a,b), in order to uniquely estimate the latitude, longitude, and depth of the corresponding scatterer. Since the amplitude of PKPbc is generally much larger than that of PKPab, it is often assumed that most of the scattering originates on the bc branch. However, until now, it was not possible to demonstrate that explicitly.

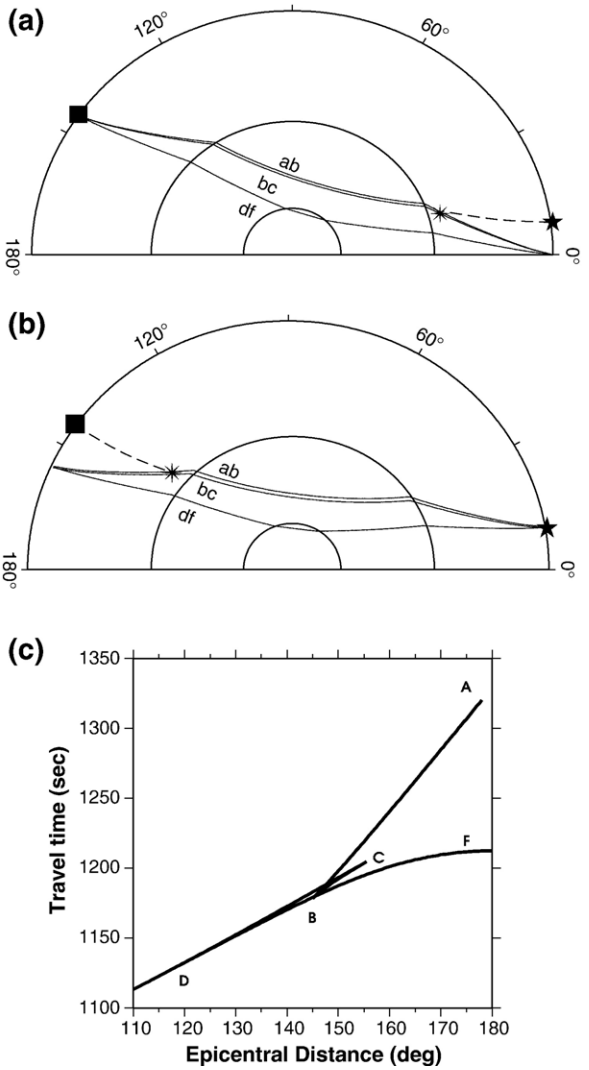

Fig. 1. (a) Schematic scattering of P to PKPbc and PKPab on the source side. The black star and square denote the event and the array, respectively. Direct P wave (the dashed line) is converted into PKP waves at the mantle scatterer. The solid lines are the PKP phases with an epicentral distance near the B caustic. (b) Schematic scattering of PKPbc and PKPab to P on the receiver side. Scattered phases arrive earlier than PKPdf in the epicentral distance range of 120° to 140° because of the much lower velocities in the core than in the mantle. (c) PKP travel time curves for ab, bc, cd, and df branches based on the ak135 model [26]. PKPab and PKPbc appear simultaneouly in the epicentral distance range between B and C caustics.

Doublet events, for which hypocenters, moment tensors, and source time history are basically identical, provide a powerful means to estimate repeatability of measurements of precursor slowness and back-azimuth. Fortunately, a very high quality earthquake doublet was reported recently [21]. Highly similar waveforms were recorded at 102 stations with a broad coverage of

epicentral distances and azimuths, and the hypocenter separation of the two events was estimated to be less than 1.0 km. Further evidence of the unique quality of this doublet was obtained from the analysis of PP phases, which have identical waveforms in a time interval of at least 70 s, and well into the PP coda [22]. In this paper, we use this doublet to conduct array analyses of PKP precursors. Taking advantage of an effective stacking technique, we obtain clear and isolated doublet PKP precursors, which, we will argue, originate from individual scatterers in the mantle. The stability of the estimated slowness and back-azimuth enable us to obtain reliable locations of several of these scatterers in the lower mantle.

2. Data, method, and results

The high quality short-period Yellowknife Seismograph Array (YK) is a long-term primary array in the International Monitoring System (IMS) seismic network, acting as the backbone facility for nuclear explosion monitoring. The epicentral distance from YK to the doublet (1993.12.01.00:59:01.2, m_b=5.5, depth=33 km; 2003.09.06.15:46:59.9, m_b=5.6, depth=33 km in the PDE catalog) at SSI is ~137.8°. 18 of all 19 stations at YK recorded very high signal-to-noise PKP precursors for both events. In order to enhance the precursor signals [23], we filtered the original seismograms in the frequency range of 1 to 2 Hz. Before stacking, we aligned traces with respect to PKIKP phases by means of cross-correlation and performed array-sided travel time corrections to remove the influence of heterogeneities just beneath the seismic array. We applied two different stacking methods: linear stacking (Fig. 2a) and Phase-Weighted Stacking (PWS) [24] (Fig. 2b).

In the case of linear stacking, which was used in previous studies [2–5], the stacked waveforms are the linear average of individual traces. It is apparent that waveforms of the doublet PKP precursors are very consistent, but they cannot be separated (Fig. 2a). In the case of PWS stacking, weights are applied to the linear stack at every sampling point [24]. The weights reflect the signal coherency in every trace. The PWS stacking technique can help us minimize the incoherent noise. Only the coherent signals of PKP precursors (A, B, C, D, and E in Fig. 2b) remain after PWS stacking. From the original design of the method, we expect that the waveform distortion from the PWS stacking will be insignificant since signals should be stationary in phase over the entire waveform, unlike for other non-linear stacking methods, such as *n*-root stacking. We had previously verified this through synthetic experiments on the weak inner core shear phase PKJKP [25].

We thus extract three well-isolated PKP precursors from the PWS stacks (A, B, and C) for both events in the doublet. Two additional, longer precursor trains, D and E, will also be discussed. The arrival times of all five precursors are very similar for both events, as are the waveforms for precursors A, B, C and for the first part of precursors D and E. An important feature of stacked waveforms of the reference PKIKP phase is that its amplitude for the 2003 event are slightly larger than for the 1993 event, reflecting the slightly larger magnitude of the 2003. The stacked waveforms of precursor B match those of PKIKP not only in amplitude relation and shape but also in time duration. This implies that the energy of precursor B is most likely scattered once from an individual scatterer in the mantle and it is not significantly contaminated by background noise or other weaker precursors. The stacked waveforms of precursor C are compatible with PKIKP in shape and time

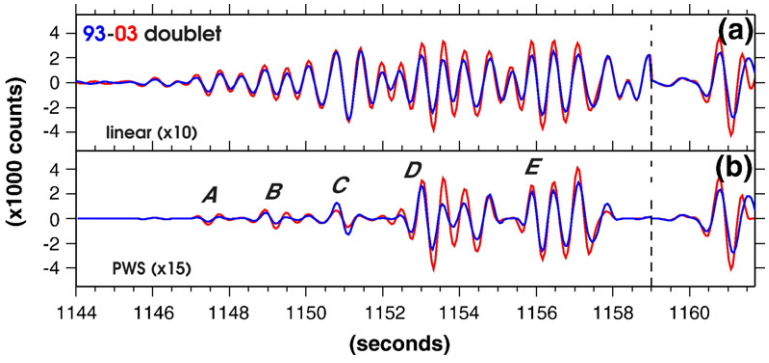

Fig. 2. Stacked waveforms of 1993 (blue) and 2003 (red) doublet events filtered between 1 and 2 Hz. (a) Linear stacking. Waveforms before the dashed line are amplified 10 times. PKP precursor train is apparent, but all precursors are mixed together. (b) Phase Weighted Stacking (PWS). Waveforms before the dashed line are amplified 15 times. Individual precursors A, B, and C stand out. Precursors D and E are likely a mixture of scattered energy arriving sequentially from multiple scatterers. The PKIKP phase arrives after the dashed line.

duration, too, but their amplitudes are anomalous: the amplitude of the PWS stacked waveform for the 2003 event is significantly smaller than that for the 1993 event. Some additional perturbation affects precursor C, and, as we will see later, this prevents us from measuring its slowness as precisely as for the other precursors. Waveforms of precursor A have a phase shift with respect to PKIKP and precursors B and C, and the likely cause will also be discussed later.

The most serious uncertainty in the measurements of slowness and back-azimuth based on a seismic array arises from signal interference. If two or more signals, which have distinct slownesses and back-azimuths, arrive at the same time, it is impossible to obtain correct estimates. This has been the case in previous precursor studies, where individual precursors were not isolated. The isolated doublet precursors in Fig. 2b not only give us more confidence in measuring their slownesses and back-azimuths but also enable us to estimate the repeatability of our measurements. In addition, encouraged by the high similarity of the first cycles in the waveforms of precursor D and E to the one of PKIKP, we also try to measure the slownesses and back-azimuths of the first arriving phases in precursor D and E.

We calculate vespagrams (Fig. 3) for PKIKP and each PKP precursor. Slownesses and back-azimuths are measured from the energy maxima for each precursor and each of the two events in the doublet. Using this method, we can obtain precise measurements of slownesses 1.85 s/deg (reading error is ~0.05 s/deg) and back-azimuths 126.5° (reading error is ~0.1°) of the PKIKP phase in the doublet, and we verify that they are very consistent with the theoretical slowness (1.84 s/deg) and back-azimuth (126.4°) computed using the ak135 seismic reference model [26]. The measured slownesses and back-azimuths are very consistent for the doublet precursors (Fig. 4). The differences between the two events range from 0.03 s/deg to 0.12 s/deg for the slowness and from 0.3° to 2.7° for the back-azimuth, respectively. It is striking that the energy of the strongest precursors D and E does not come from the great circle

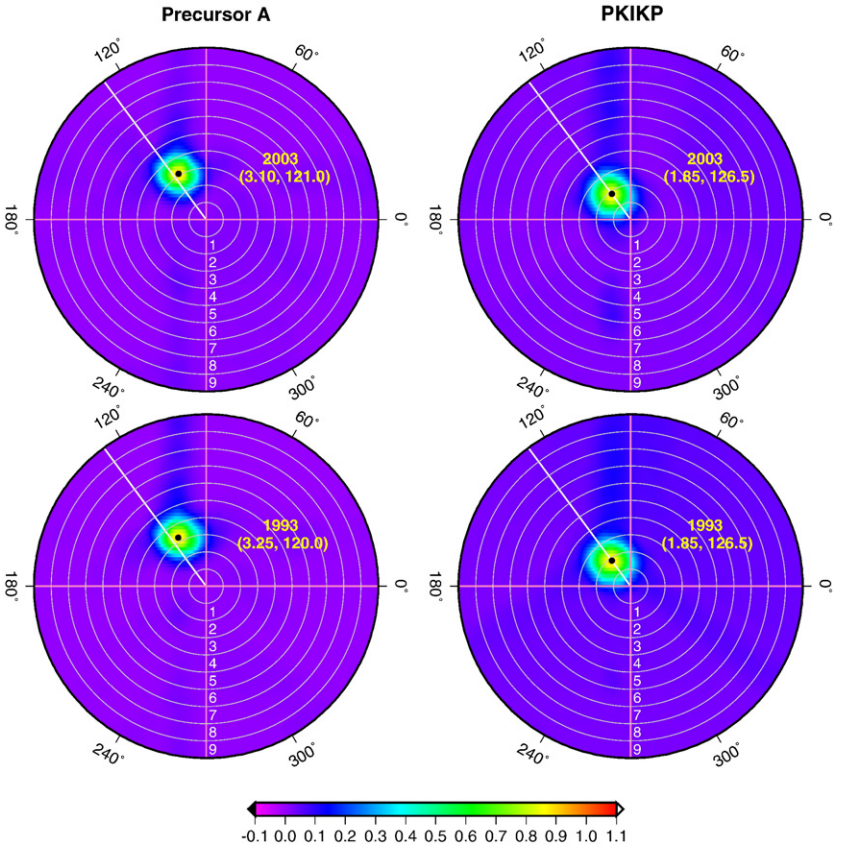

Fig. 3. Vespagrams of PKIKP (right panel) and PKP precursor A (left panel) for the 2003 (top) and 1993 (bottom) events, in the slowness and back-azimuth domain. Solid white lines denote the event back-azimuth (126.4°). Grey circles denote the scale of slowness with an interval of 1.0 s/deg. In yellow brackets are estimates of slowness (s/deg) and back-azimuth (degree), respectively. The theoretical slowness of PKIKP is 1.84 s/deg.

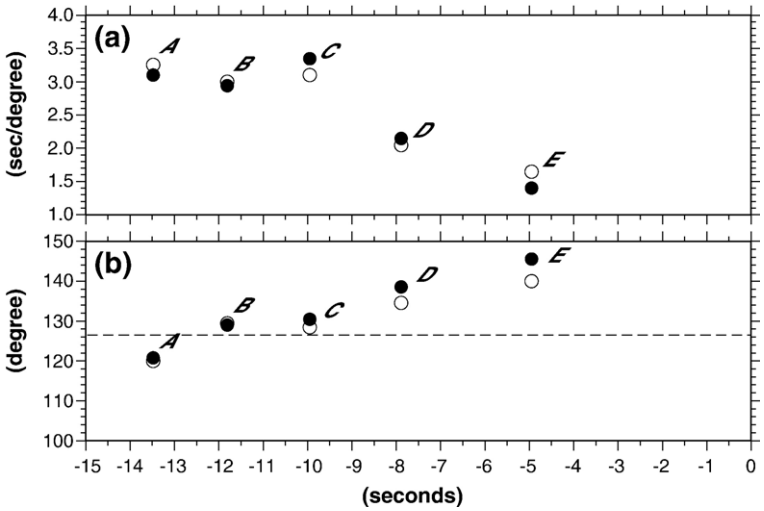

Fig. 4. Measured slownesses (a) and back-azimuths (b) from vespagrams for precursor A, B, C, D, and E as a function of the arrival time with respect to PKIKP. Solid dots and open circle correspond to the 2003 and 1993 events, respectively. The measured of slownesses (s/deg) and back-azimuths (deg) are A (3.10, 3.25; 120.8, 120.0), B (2.94, 3.00; 129.0, 129.6), C (3.35, 3.11; 130.5, 128.5), D (2.15, 2.05; 139.0, 134.0), and E (1.40, 1.64; 140.0, 145.4). The average differences in estimated slowness and back-azimuth are 0.08 s/deg and 1.4 deg, respectively. The dashed line in (b) is the theoretical back-azimuth of the doublet. Differential arrival times are measured from precursor and PKIKP envelope peaks, with an uncertainty of less than 0.1 s.

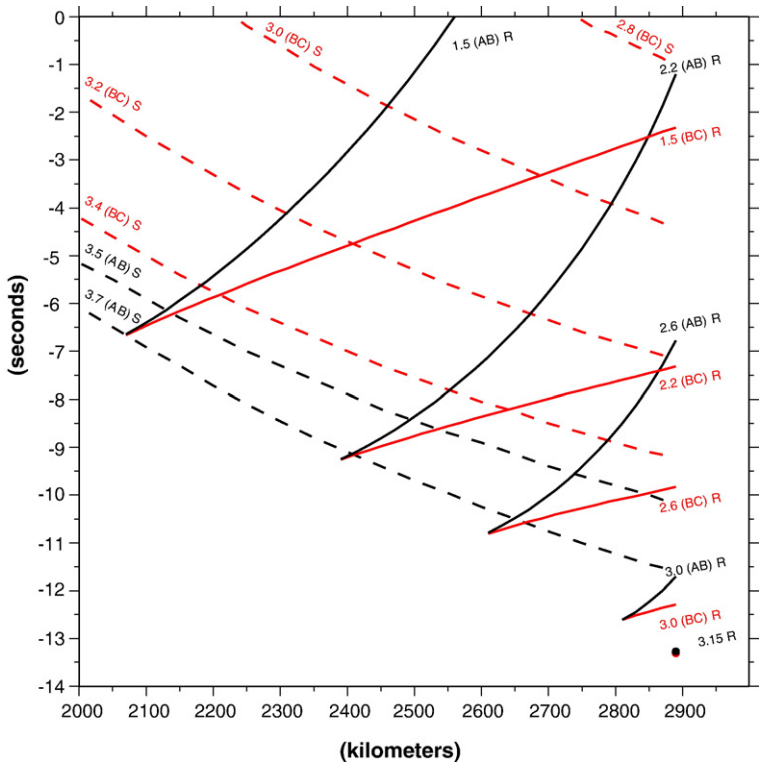

Fig. 5. Differential arrival times of PKP precursors with respect to PKIKP as a function of the scatterer depth in the great circle plane. Here negative arrival times mean that precursors arrive earlier than PKIKP. Solid lines correspond to the receiver-side scattering (PKP-to-P) of PKPbc (red) and PKPab (black) for different P wave slownesses; Dashed lines correspond to the source-side scattered (P-to-PKP) PKPbc (red) and PKPab (black) for different PKP wave slownesses.

plane. The corresponding back-azimuth deviation is as large as ~16 (precursor E).

Based on ray tracing and the single-scattering assumption [9,23,27], we are able to locate the scattering regions responsible for the individual PKP precursors, using our precise measurements of slownesses, back-azimuths, and differential arrival times. In the great circle plane from the sources to the receivers, only slownesses and differential arrival times of the precursors are required to locate the mantle scatterer depths (Fig. 5). First of all, we need to determine whether the precursors are from the receiver side or from the source side according to the measured slowness. On the receiver side, the measured slowness should be less than ~3.2 s/deg. On the source side, the measured slowness should be larger than ~3.0 s/deg if the corresponding precursor arrives over 3.5 s earlier than PKIKP, and the measured slowness should be larger than ~3.7 s/deg if the corresponding precursor arrives over 11.0 s earlier than PKIKP.

The arrival time of precursor A is 13.48 s earlier than PKIKP and its measured slownesses are 3.10 s/deg (2003) and 3.25 s/deg (1993), so precursor A must be scattered on the receiver side. The arrival time of precursor B is 11.81 s and its measured slowness are 2.94 s/deg (2003) and 3.00 s/deg (1993), so precursor B must also be scattered on the receiver side. Similarly, precursor D (7.89 s, 2.15 s/deg (2003) and 2.05 s/deg (1993)) and E (4.95 s, 1.40 s/deg (2003) and 1.64 s/deg (1993)) are also scattered on the receiver side.

For precursor C (9.95 s, 3.35 s/deg (2003) and 3.11 s/deg (1993)), we cannot make an unambiguous judgment: taking into account the relatively larger uncertainty of its measured slowness, if it is on the receiver side, its arrival time should be over 12.5 s earlier than PKIKP; if it is on the source side, its arrival time cannot be 8.0 s earlier than PKIKP. Because we are using differential travel times of the precursors with respect to the PKIKP phases and their ray paths are arguably close, the uncertainty caused by heterogeneities in the crust and mantle cannot be as large as 2.0 s. A likely scenario is that precursor C corresponds to a more complex scattering surface, but we cannot rule out the possibility that precursor C may originate on the source side.

After confirming that precursors A, B, D, and E are scattered on the receiver side, we have to determine whether they are scattered from PKPbc or PKPab phases. Indeed, even if the slowness and the arrival time

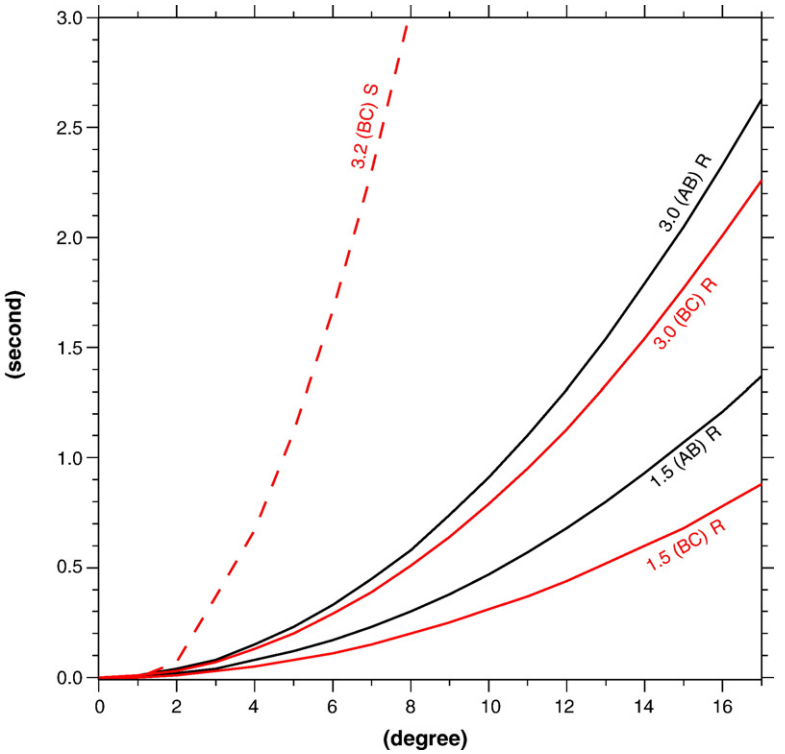

Fig. 6. Influence of back-azimuth deviations on arrival times of precursors. The horizontal axis is the back-azimuth deviation with respect to the great circle from the source (at SSI) to receiver (YK), and the vertical axis is the resulting delay time. Solid lines correspond to the receiver-side scattering of PKPbc (red) and PKPab (black) with various values of slownesses; the dashed line corresponds to a source-side scattering of PKPbc.

are the same, the scatterer depth may be different depending on whether it originates from PKPbc or PKPab. For the smaller slowness (e.g., precursor E), the depth difference can be more than 100 km. By comparison of stacked waveforms between PKP precursors and PKIKP, the similarity of precursor B, D, E and PKIKP suggests that these precursors should be scattered from PKPbc phases rather than PKPab phases. Otherwise, their waveforms would most likely have significant (~90°) phase shifts with respect to the PKIKP phases. Precursor A is special. Scattered energy from PKPbc and PKPab arrives at the nearly same time (Fig. 5), and so it is not surprising that its doublet waveforms are phase shifted from that of PKIKP.

Before we can determine coordinates and depths of the individual scatterers for the PKP precursors, we have to do corrections for the back-azimuth deviations, too (Fig. 6). The back-azimuth deviation can delay the arrival of the PKP precursor. If the deviation with respect to the great circle plane is less than 4°, the resulting time delay is not significant (less than 0.1 s). Otherwise, the resulting time delay can become important.

Comprehensive consideration of the high quality differential arrival times, slowness, and back-azimuth deviations enables us to locate the mantle scatterers for precursors A, B, D, and E (Fig. 7). Precursors A and B are scattered at the CMB, while precursors D and E are scattered at ~420 km and ~620 km above the CMB, respectively.

3. Discussion

The high quality doublet events give us a unique opportunity to estimate the stability of our methodology for locating small-scale heterogeneities in the mantle. The average difference in back-azimuths (±1.4°) can affect our estimates of scatterer coordinates at a level of ~0.6°, but it does not affect our estimates of scatterer depths. The average difference in slowness (±0.08 s/deg) can affect our estimates both of coordinates and of

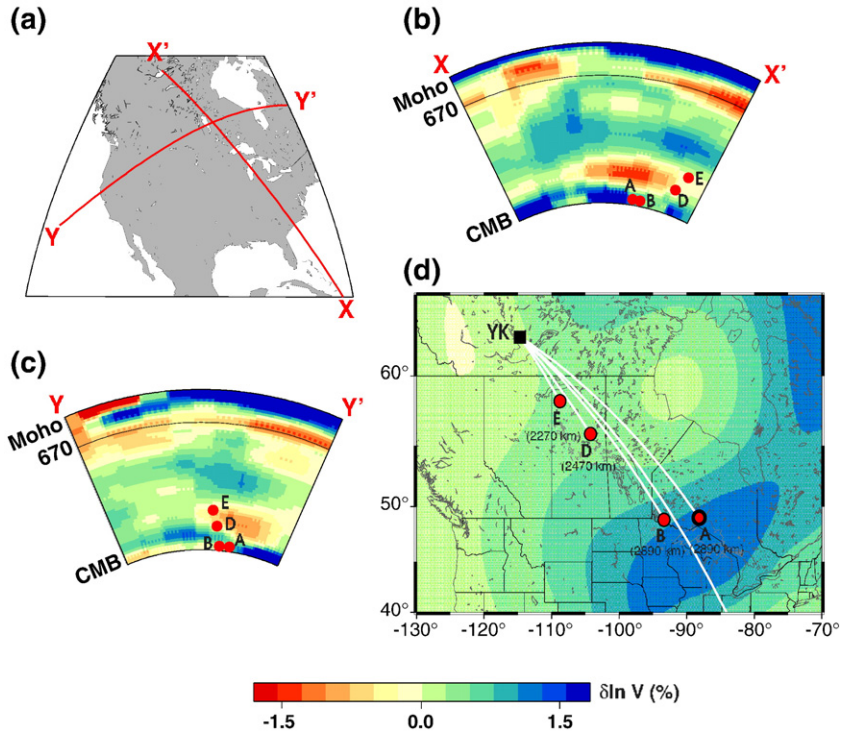

Fig. 7. Distribution of seismic scatterers in the lower mantle. (a) Map view indicating the location of two vertical profiles in the region of our study. (b) and (c) Vertical cross-sections of the SAW24B16 shear wave tomographic model [30]. Profile XX' is along the great circle containing source and receivers, and profile YY' is perpendicular to it. Red dots show the projected locations of our constrained mantle scatterers into the cross-sections. In the region of higher than average velocity in the lower mantle to the west of the scatterers corresponds to a feature in the model by Ren et al. [29] which these authors associated with the fossil Farallon slab. (d) Map view of the distribution of seismic scatterers in the lower mantle. Black square denotes the Yellowknife seismic arry (YK). Red dots indicate our located scatterers. Solid white lines are the horizontal projections of the ray paths of precursors, and the corresponding scattering angles are 45.8°, 42.1°, 24.4°, and 16.0° for scatterer A, B, D, and E, respectively. The dashed white line is part of the great circle from the sources in South Sandwich Islands (SSI) to YK. The background tomographic model shows the distribution of shear-wave velocity at a depth of 2800 km [30].

depths. The resulting influence on the coordinates is ~±0.5°, and the resulting influence on the depth is ~±70 km, respectively.

In addition to uncertainties in slowness and back-azimuths, there may be a systematic error related to the selected seismic reference model. All of our theoretical calculations (Figs. 5–7) are based on model ak135 [26]. Any significant perturbation of P-wave velocity in the region of our study with respect to this model would result in systematic errors between the theoretical and the measured (Fig. 4) differential arrival times of the PKP precursors. And this would deteriorate the precision of the located mantle scatterers. Here we estimate this systematic error by comparison of the predicted and observed arrival times of PKIKP phases. We calculate the theoretical arrival times of PKIKP phases for each trace based on model ak135. The differences between the predicted arrival times and the measured arrival times are small (<0.2 s). On the other hand, we are working with differential arrival times between PKIKP and the precursors. In the mantle and crust, their ray paths are arguably close. Therefore, the systematic error associated with our selected seismic reference model should be less than 0.2 s. And the resulting error in the scatterer depths is less than 40 km.

Except for the distorted PKP precursor C, the measured slownesses steadily decrease when the precursors approach the PKIKP phases (Fig. 4a). At the same time, the constrained heights (above the CMB) of the corresponding scatterers increase significantly (Fig. 7). This is consistent with previous studies [6,23]. Scattered energy at a higher level above the CMB arrives later in the precursor train. When the scatterer arises along the PKPbc (or PKPab) ray path on the receiver side (Fig. 1b), the incident angle of the scattered P wave beneath the array decreases and so its slowness decreases. Therefore, in order to detect the highest scatterers above the CMB, one should search for isolated PKP precursors arriving close to PKIKP phases in a broad epicentral distance range from 120° to 140°.

Based on the model with small-scale (~8 km), weak velocity perturbations (1%), and uniformly distributed random heterogeneities through the mantle, Hedlin et al. [9] and Cormier [10] successfully modeled the average amplitudes of the PKP precursors at the global scale. Their model implies a basically continuous PKP precursor energy train, and most of the energy most likely comes from the vicinity of the great circle plane containing the source and the receiver. However, in the more local region of our study, we can observe well-isolated PKP precursors (Fig. 2b) and some of the corresponding energy arrives significantly outside of the great circle plane (Figs. 4b and 7d). Therefore, the local small-scale heterogeneity structure beneath western North America is likely different from the suggested global model. There may be some stronger mantle scatterers in this region, as Hedlin and Shearer pointed out on basis of the inversion of PKP precursors [20]. Scattered PKP precursors from the stronger scatterers should be able to keep the coherency of their signals better than those from the weaker scatterers which are more affected by background noise when they arrive at the seismic array. Thus, there may be other scatterers hidden in the wavetrains, but only the strongest stand out after the PWS stacking. On the other hand, the fact that we can identify isolated scatterers with waveforms generally so similar to the reference PKIKP phase suggests that the scatterers are spatially extended at a scale length longer than the incident wavelength. To confirm this would require a broadband analysis of frequency dependence.

Most previous attempts at locating scatterers in the lower mantle have associated those with ultra-low velocity zones [15–19]. However, the site of our scatterers, western North America, has been associated with subduction zones for at least the past ~100 millions of years [28]. Ren et al. [29] have recently proposed how the history of subduction under north America can be followed in their regional high resolution tomographic model. While the locations of our scatterers fall at the edge of the region where they have good resolution, we can compare them with global tomography models. First, we note that the depths of our mantle scatterers increase from 2270 km (precursor E) to 2890 km (precursor A and B at the CMB), and the corresponding dipping angle is ~20° (Fig. 7), consistent with the dip direction expected for subduction and fossil subduction in this region. Scatterers A and B are located in a high velocity region near the CMB (Fig. 7b–d). Scatterers D and E are located at a transition region from high to low velocities (Fig. 7b,c), which is consistently mapped in mantle tomography models [30–32]. This suggests that the scatterers may be related to the sharp and irregular boundary of the slab remnants beneath north America [9,10] and implies that subducted slabs that have penetrated deep into the lower mantle may have retained their distinct compositional signature all the way to the CMB, in support of recent geodynamical modeling [33].

Given that we now have an idea of the accuracy of our method to locate mantle scatterers using doublet PKP precursors, we can apply the method to single events in the future. The number of quality doublets is very limited [21], but high quality single events are well distributed. In a broad coverage of epicentral distance

range (120° to 140°) and back-azimuth, we should have better conditions to constrain the horizontal and vertical distribution of mantle scatterers and to provide more detailed information on tectonic processes in the deep mantle at the regional scale.

4. Conclusions

Array analysis of PKP precursors from a high quality doublet event, recorded at Yellowknife, allows us to locate individual scatterers in the lower mantle beneath western Canada. These scatterers are likely of significant spatial extent (several tens of kilometers at least) to produce coherent arrivals and stable waveforms as observed here. We suggest that they are associated with the remnants of subducting slabs beneath northwestern North America, in which case these slabs would have retained their compositional signature for many millions of years, as predicted by geodynamical modelling. We have shown that the locations of the scatterers are sufficiently accurate to warrant future application of this methodology to precursors from single earthquakes. This will result in a much larger dataset, which will help delineate structures with sharp irregular boundaries in the lower mantle, contributing to our understanding of global mantle dynamics.

Acknowledgements

We thank the operators of the Yellowknife Seismic Array and Canadian National Seismograph Network. We are grateful to Peter Shearer and an anonymous reviewer for their constructive comments. This work was supported by NSF grant EAR-0308750. This is Berkeley Seismological Laboratory Contribution #06-15.

References

[1] B. Gutenberg, C.F. Richter, On seismic waves: I, Gerlands Beitr. Z. Geophys. 43 (1934) 56–133.
[2] J.R. Cleary, R.A. Haddon, Seismic wave scattering near the core–mantle boundary: a new interpretation of precursors to PKP, Nature 240 (1972) 549–551.
[3] D.J. Doornbos, E.S. Husebye, Array analysis of PKP phases and their precursors, Phys. Earth Planet. Int. 5 (1972) 387–399.
[4] D.J. Doornbos, N.J. Vlaar, Regions of seismic wave scattering in the Earth's mantle and precursors to PKP, Nature 243 (1973) 58–61.
[5] D.W. King, R.A. Haddon, J.R. Cleary, Array analysis of precursors to PKIKP in the distance range 128° to 142°, Geophys. J. R. Astron. Soc. 37 (1974) 157–173.
[6] D.J. Doornbos, Characteristics of lower mantle inhomogeneities from scattered waves, Geophys. J. R. Astron. Soc. 44 (1976) 447–470.
[7] B.A. Bolt, Gutenberg's early PKP observations, Nature 196 (1962) 122–124.
[8] I.S. Sacks, G. Saa, The structure of the transition zone between the inner core and the outer core, Carnegie Institution Year Book, Washington, 1969–1970, pp. 419–426.
[9] M.A. Hedlin, P.M. Shearer, P.S. Earle, Seismic evidence for small-scale heterogeneity throughout the Earth's mantle, Nature 387 (1997) 145–150.
[10] V.F. Cormier, Anisotropy of heterogeneity scale lengths in the lower mantle from PKIKP precursors, Geophys. J. Int. 136 (1999) 373–384.
[11] L. Margerin, G. Nolet, Multiple scattering of high-frequency seismic waves in the deep Earth: PKP precursor analysis inversion for mantle granularity, J. Geophys. Res. 108 (2003) 2514.
[12] M. Gurnis, G.F. Davies, Mixing in numerical models of mantle convection incorporating plate tectonics, J. Geophys. Res. 91 (1986) 6375–6395.
[13] G.F. Davies, Mantle plumes, mantle stirring and hotspot chemistry, Earth Planet. Sci. Lett. 99 (1990) 94–109.
[14] U.R. Christensen, A.W. Hofman, Segregation of subducted oceanic crust in the convecting mantle, J. Geophys. Res. 99 (1994) 19867–19884.
[15] L. Wen, D. Helmberger, Ultra low velocity zones near the core–mantle boundary from broadband PKP precursors, Science 279 (1998) 1701–1703.
[16] C. Thomas, M. Weber, C.W. Wicks, F. Scherbaum, Small scatters in the lower mantle observed at German broadband arrays, J. Geophys. Res. 104 (1999) 15073–15088.
[17] L. Wen, Intense seismic scattering near the core–mantle boundary beneath the Comoros hotspot, Geophys. Res. Lett. 27 (2000) 3627–3630.
[18] F. Niu, L. Wen, Strong seismic scatters near the core–mantle boundary west of Mexico, Geophys. Res. Lett. 28 (2001) 3557–3560.
[19] J. Vidale, M. Hedlin, Evidence of the partial melt at the core–mantle boundary north of Tonga from strong scattering of seismic waves, Nature 391 (1998) 682–684.
[20] M. Hedlin, P. Shearer, An analysis of large-scale variations in small-scale mantle heterogeneity using Global Seismographic Network recordings of precursors to PKP, J. Geophys. Res. 105 (2000) 13655–13673.
[21] J. Zhang, X. Song, Y. Li, P.G. Richards, X. Sun, F. Waldhauser, Inner core differential motion confirmed by earthquake waveform doublets, Science 309 (2005) 1357–1360.
[22] A. Cao, Y. Masson, B. Romanowicz, Short wavelength topography on the inner core boundary, Proc. Natl. Acad. Sci. U.S.A. 104 (2007) 31–35.
[23] V.F. Cormier, Time-domain modelling of PKIKP precursors for constraints on the heterogeneity in the lowermost mantle, Geophys. J. Int. 121 (1995) 725–736.
[24] M. Schimmel, H. Paulssen, Noise reduction and the detection of weak, coherent signals through phase-weighted stacks, Geophys. J. Int. 130 (1997) 497–505.
[25] A. Cao, B. Romanowicz, N. Takeuchi, An observation of PKJKP: inferences on inner core shear proprieties, Science 308 (2005) 1453–1455.
[26] B.L.N. Kennett, E.R. Engdahl, R. Buland, Constraints on seismic velocities in the Earth from travel times, Geophys. J. Int. 122 (1995) 108–124.
[27] D.J. Doornbos, Multiple scattering by topographic relief with application to the core–mantle boundary, Geophys. J. Int. 92 (1988) 465–478.

[28] T. Atwater, Plate tectonic history of the northeast Pacific and western North America, in: E.L. Winterer, D.M. Hussong, R.W. Decker (Eds.), The Geology of North America, Vol. N. Geol. Soc. Am., Boulder, CO, , 1989, pp. 21–72.
[29] Y. Ren, E. Stutzmann, R. van der Hilst, J. Besse, Understanding seismic heterogeneities in the lower mantle beneath the Americas from seismic tomography and plate tectonic history, J. Geophys. Res., in press.
[30] C. Megnin, B. Romanowicz, The three-dimensional shear velocity structure of the mantle from the inversion of body, surface and higher-mo de waveforms, Geophys. J. Int. 143 (2000) 709–728.
[31] Y. Gu, A. Dziewonski, W. Su, G. Ekstrom, Models of the mantle shear velocity and discontinuities in the pattern of lateral heterogeneities, J. Geophys. Res. 106 (2001) 11,169–11,199.
[32] J. Ritsema, H.J. van Heijst, J.H. Woodhouse, Global transition zone tomography, J. Geophys. Res. 109 (2004) 14.
[33] E. Tan, M. Gurnis, L. Han, Slabs in the lower mantle and their modulation of plume formation, Geochem. Geophys. Geosyst. 3 (2002) 1067.